

Search for the Associated Production of a b Quark and a Neutral Supersymmetric Higgs Boson that Decays into τ Pairs

V. M. Abazov,³⁷ B. Abbott,⁷⁵ M. Abolins,⁶⁵ B. S. Acharya,³⁰ M. Adams,⁵¹ T. Adams,⁴⁹ E. Aguiló,⁶ M. Ahsan,⁵⁹ G. D. Alexeev,³⁷ G. Alkhazov,⁴¹ A. Alton,^{64,*} G. Alverson,⁶³ G. A. Alves,² L. S. Anzu,³⁶ M. Aoki,⁵⁰ Y. Arnould,¹⁴ M. Arov,⁶⁰ A. Askew,⁴⁹ B. Ásman,⁴² O. Atramentov,^{49,†} C. Avila,⁸ J. BackusMayes,⁸² F. Badaud,¹³ L. Bagby,⁵⁰ B. Baldin,⁵⁰ D. V. Bandurin,⁵⁹ S. Banerjee,³⁰ E. Barberis,⁶³ A.-F. Barfuss,¹⁵ P. Baringer,⁵⁸ J. Barreto,² J. F. Bartlett,⁵⁰ U. Bassler,¹⁸ D. Bauer,⁴⁴ S. Beale,⁶ A. Bean,⁵⁸ M. Begalli,³ M. Begel,⁷³ C. Belanger-Champagne,⁴² L. Bellantoni,⁵⁰ J. A. Benitez,⁶⁵ S. B. Beri,²⁸ G. Bernardi,¹⁷ R. Bernhard,²³ I. Bertram,⁴³ M. Besançon,¹⁸ R. Beuselinck,⁴⁴ V. A. Bezzubov,⁴⁰ P. C. Bhat,⁵⁰ V. Bhatnagar,²⁸ G. Blazey,⁵² S. Blessing,⁴⁹ K. Bloom,⁶⁷ A. Boehlein,⁵⁰ D. Boline,⁶² T. A. Bolton,⁵⁹ E. E. Boos,³⁹ G. Borissov,⁴³ T. Bose,⁶² A. Brandt,⁷⁸ R. Brock,⁶⁵ G. Brooijmans,⁷⁰ A. Bross,⁵⁰ D. Brown,¹⁹ X. B. Bu,⁷ D. Buchholz,⁵³ M. Buehler,⁸¹ V. Buescher,²⁵ V. Bunichev,³⁹ S. Burdin,^{43,‡} T. H. Burnett,⁸² C. P. Buszello,⁴⁴ P. Calfayan,²⁶ B. Calpas,¹⁵ S. Calvet,¹⁶ E. Camacho-Pérez,³⁴ J. Cammin,⁷¹ M. A. Carrasco-Lizarraga,³⁴ E. Carrera,⁴⁹ W. Carvalho,³ B. C. K. Casey,⁵⁰ H. Castilla-Valdez,³⁴ S. Chakrabarti,⁷² D. Chakraborty,⁵² K. M. Chan,⁵⁵ A. Chandra,⁵⁴ E. Cheu,⁴⁶ S. Chevalier-Théry,¹⁸ D. K. Cho,⁶² S. W. Cho,³² S. Choi,³³ B. Choudhary,²⁹ T. Christoulias,⁴⁴ S. Cihangir,⁵⁰ D. Claes,⁶⁷ J. Clutter,⁵⁸ M. Cooke,⁵⁰ W. E. Cooper,⁵⁰ M. Corcoran,⁸⁰ F. Couderc,¹⁸ M.-C. Cousinou,¹⁵ D. Cutts,⁷⁷ M. Ćwiok,³¹ A. Das,⁴⁶ G. Davies,⁴⁴ K. De,⁷⁸ S. J. de Jong,³⁶ E. De La Cruz-Burelo,³⁴ K. DeVaughan,⁶⁷ F. Déliot,¹⁸ M. Demarteau,⁵⁰ R. Demina,⁷¹ D. Denisov,⁵⁰ S. P. Denisov,⁴⁰ S. Desai,⁵⁰ H. T. Diehl,⁵⁰ M. Diesburg,⁵⁰ A. Dominguez,⁶⁷ T. Dorland,⁸² A. Dubey,²⁹ L. V. Dudko,³⁹ L. Duflot,¹⁶ D. Duggan,⁴⁹ A. Duperrin,¹⁵ S. Dutt,²⁸ A. Dyshkant,⁵² M. Eads,⁶⁷ D. Edmunds,⁶⁵ J. Ellison,⁴⁸ V. D. Elvira,⁵⁰ Y. Enari,¹⁷ S. Eno,⁶¹ H. Evans,⁵⁴ A. Evdokimov,⁷³ V. N. Evdokimov,⁴⁰ G. Facini,⁶³ A. V. Ferapontov,⁷⁷ T. Ferbel,^{61,71} F. Fiedler,²⁵ F. Filthaut,³⁶ W. Fisher,⁵⁰ H. E. Fisk,⁵⁰ M. Fortner,⁵² H. Fox,⁴³ S. Fuess,⁵⁰ T. Gadfort,⁷⁰ C. F. Galea,³⁶ A. Garcia-Bellido,⁷¹ V. Gavrilov,³⁸ P. Gay,¹³ W. Geist,¹⁹ W. Geng,^{15,65} D. Gerbaudo,⁶⁸ C. E. Gerber,⁵¹ Y. Gershtein,^{49,†} D. Gillberg,⁶ G. Ginther,^{50,71} G. Golovanov,³⁷ B. Gómez,⁸ A. Goussiou,⁸² P. D. Grannis,⁷² S. Greder,¹⁹ H. Greenlee,⁵⁰ Z. D. Greenwood,⁶⁰ E. M. Gregores,⁴ G. Grenier,²⁰ Ph. Gris,¹³ J.-F. Grivaz,¹⁶ A. Grohsjean,¹⁸ S. Grünenwald,⁵⁰ M. W. Grünewald,³¹ F. Guo,⁷² J. Guo,⁷² G. Gutierrez,⁵⁰ P. Gutierrez,⁷⁵ A. Haas,^{70,§} P. Haefner,²⁶ S. Hagopian,⁴⁹ J. Haley,⁶³ I. Hall,⁶⁵ R. E. Hall,⁴⁷ L. Han,⁷ K. Harder,⁴⁵ A. Harel,⁷¹ J. M. Hauptman,⁵⁷ J. Hays,⁴⁴ T. Hebbeker,²¹ D. Hedin,⁵² J. G. Hegeman,³⁵ A. P. Heinson,⁴⁸ U. Heintz,⁶² C. Hensel,²⁴ I. Heredia-De La Cruz,³⁴ K. Herner,⁶⁴ G. Hesketh,⁶³ M. D. Hildreth,⁵⁵ R. Hirosky,⁸¹ T. Hoang,⁴⁹ J. D. Hobbs,⁷² B. Hoeneisen,¹² M. Hohlfeld,²⁵ S. Hossain,⁷⁵ P. Houben,³⁵ Y. Hu,⁷² Z. Hubacek,¹⁰ N. Huske,¹⁷ V. Hynek,¹⁰ I. Iashvili,⁶⁹ R. Illingworth,⁵⁰ A. S. Ito,⁵⁰ S. Jabeen,⁶² M. Jaffré,¹⁶ S. Jain,⁷⁵ K. Jakobs,²³ D. Jamin,¹⁵ R. Jesik,⁴⁴ K. Johns,⁴⁶ C. Johnson,⁷⁰ M. Johnson,⁵⁰ D. Johnston,⁶⁷ A. Jonckheere,⁵⁰ P. Jonsson,⁴⁴ A. Juste,⁵⁰ E. Kajfasz,¹⁵ D. Karmanov,³⁹ P. A. Kasper,⁵⁰ I. Katsanos,⁶⁷ V. Kaushik,⁷⁸ R. Kehoe,⁷⁹ S. Kermiche,¹⁵ N. Khalatyan,⁵⁰ A. Khanov,⁷⁶ A. Kharchilava,⁶⁹ Y. N. Kharzeev,³⁷ D. Khatidze,⁷⁷ M. H. Kirby,⁵³ M. Kirsch,²¹ J. M. Kohli,²⁸ A. V. Kozelov,⁴⁰ J. Kraus,⁶⁵ A. Kumar,⁶⁹ A. Kupco,¹¹ T. Kurča,²⁰ V. A. Kuzmin,³⁹ J. Kvita,⁹ F. Lacroix,¹³ D. Lam,⁵⁵ S. Lammers,⁵⁴ G. Landsberg,⁷⁷ P. Lebrun,²⁰ H. S. Lee,³² W. M. Lee,⁵⁰ A. Leflat,³⁹ J. Lellouch,¹⁷ L. Li,⁴⁸ Q. Z. Li,⁵⁰ S. M. Liotti,⁵ J. K. Lim,³² D. Lincoln,⁵⁰ J. Linnemann,⁶⁵ V. V. Lipaev,⁴⁰ R. Lipton,⁵⁰ Y. Liu,⁷ Z. Liu,⁶ A. Lobodenko,⁴¹ M. Lokajicek,¹¹ P. Love,⁴³ H. J. Lubatti,⁸² R. Luna-Garcia,^{34,||} A. L. Lyon,⁵⁰ A. K. A. Maciel,² D. Mackin,⁸⁰ P. Mättig,²⁷ R. Magaña-Villalba,³⁴ P. K. Mal,⁴⁶ S. Malik,⁶⁷ V. L. Malyshov,³⁷ Y. Maravin,⁵⁹ B. Martin,¹⁴ J. Martínez-Ortega,³⁴ R. McCarthy,⁷² C. L. McGivern,⁵⁸ M. M. Meijer,³⁶ A. Melnitchouk,⁶⁶ L. Mendoza,⁸ D. Menezes,⁵² P. G. Mercadante,⁴ M. Merkin,³⁹ A. Meyer,²¹ J. Meyer,²⁴ N. K. Mondal,³⁰ R. W. Moore,⁶ T. Moulik,⁵⁸ G. S. Muanza,¹⁵ M. Mulhearn,⁸¹ O. Mundal,²² L. Mundim,³ E. Nagy,¹⁵ M. Naimuddin,²⁹ M. Narain,⁷⁷ R. Nayyar,²⁹ H. A. Neal,⁶⁴ J. P. Negret,⁸ P. Neustroev,⁴¹ H. Nilsen,²³ H. Nogima,³ S. F. Novaes,⁵ T. Nunnemann,²⁶ G. Obrant,⁴¹ D. Onoprienko,⁵⁹ J. Orduna,³⁴ N. Osman,⁴⁴ J. Osta,⁵⁵ R. Otec,¹⁰ G. J. Otero y Garzón,¹ M. Owen,⁴⁵ M. Padilla,⁴⁸ P. Padley,⁸⁰ M. Pangilinan,⁷⁷ N. Parashar,⁵⁶ V. Parihar,⁶² S.-J. Park,²⁴ S. K. Park,³² J. Parsons,⁷⁰ R. Partridge,⁷⁷ N. Parua,⁵⁴ A. Patwa,⁷³ B. Penning,⁵⁰ M. Perfilov,³⁹ K. Peters,⁴⁵ Y. Peters,⁴⁵ P. Pétroff,¹⁶ R. Piegaia,¹ J. Piper,⁶⁵ M.-A. Pleier,⁷³ P. L. M. Podesta-Lerma,^{34,||} V. M. Podstavkov,⁵⁰ Y. Pogorelov,⁵⁵ M.-E. Pol,² P. Polozov,³⁸ A. V. Popov,⁴⁰ M. Prewitt,⁸⁰ S. Protopopescu,⁷³ J. Qian,⁶⁴ A. Quadt,²⁴ B. Quinn,⁶⁶ M. S. Rangel,¹⁶ K. Ranjan,²⁹ P. N. Ratoff,⁴³ I. Razumov,⁴⁰ P. Renkel,⁷⁹ P. Rich,⁴⁵ M. Rijssenbeek,⁷² I. Ripp-Baudot,¹⁹ F. Rizatdinova,⁷⁶ S. Robinson,⁴⁴ M. Rominsky,⁷⁵ C. Royon,¹⁸ P. Rubinov,⁵⁰ R. Ruchti,⁵⁵ G. Safronov,³⁸ G. Sajot,¹⁴ A. Sánchez-Hernández,³⁴ M. P. Sanders,²⁶ B. Sanghi,⁵⁰ G. Savage,⁵⁰ L. Sawyer,⁶⁰ T. Scanlon,⁴⁴ D. Schaile,²⁶ R. D. Schamberger,⁷² Y. Scheglov,⁴¹ H. Schellman,⁵³ T. Schliephake,²⁷ S. Schlobohm,⁸² C. Schwanenberger,⁴⁵ R. Schwienhorst,⁶⁵ J. Sekaric,⁵⁸ H. Severini,⁷⁵ E. Shabalina,²⁴ M. Shamim,⁵⁹

V. Shary,¹⁸ A. A. Shchukin,⁴⁰ R. K. Shivpuri,²⁹ V. Simak,¹⁰ V. Sirotenko,⁵⁰ P. Skubic,⁷⁵ P. Slattery,⁷¹ D. Smirnov,⁵⁵
 G. R. Snow,⁶⁷ J. Snow,⁷⁴ S. Snyder,⁷³ S. Söldner-Rembold,⁴⁵ L. Sonnenschein,²¹ A. Sopczak,⁴³ M. Sosebee,⁷⁸
 K. Soustruznik,⁹ B. Spurlock,⁷⁸ J. Stark,¹⁴ V. Stolin,³⁸ D. A. Stoyanova,⁴⁰ J. Strandberg,⁶⁴ M. A. Strang,⁶⁹ E. Strauss,⁷²
 M. Strauss,⁷⁵ R. Ströhmer,²⁶ D. Strom,⁵¹ L. Stutte,⁵⁰ S. Sumowidagdo,⁴⁹ P. Svoisky,³⁶ M. Takahashi,⁴⁵ A. Tanasijczuk,¹
 W. Taylor,⁶ B. Tiller,²⁶ M. Titov,¹⁸ V. V. Tokmenin,³⁷ I. Torchiani,²³ D. Tsybychev,⁷² B. Tuchming,¹⁸ C. Tully,⁶⁸
 P. M. Tuts,⁷⁰ R. Unalan,⁶⁵ L. Uvarov,⁴¹ S. Uvarov,⁴¹ S. Uzunyan,⁵² P. J. van den Berg,³⁵ R. Van Kooten,⁵⁴
 W. M. van Leeuwen,³⁵ N. Varelas,⁵¹ E. W. Varnes,⁴⁶ I. A. Vasilyev,⁴⁰ P. Verdier,²⁰ L. S. Vertogradov,³⁷ M. Verzocchi,⁵⁰
 M. Vesterinen,⁴⁵ D. Vilanova,¹⁸ P. Vint,⁴⁴ P. Vokac,¹⁰ R. Wagner,⁶⁸ H. D. Wahl,⁴⁹ M. H. L. S. Wang,⁷¹ J. Warchol,⁵⁵
 G. Watts,⁸² M. Wayne,⁵⁵ G. Weber,²⁵ M. Weber,^{50,**} A. Wenger,^{23,††} M. Wetstein,⁶¹ A. White,⁷⁸ D. Wicke,²⁵
 M. R. J. Williams,⁴³ G. W. Wilson,⁵⁸ S. J. Wimpenny,⁴⁸ M. Wobisch,⁶⁰ D. R. Wood,⁶³ T. R. Wyatt,⁴⁵ Y. Xie,⁷⁷ C. Xu,⁶⁴
 S. Yacoob,⁵³ R. Yamada,⁵⁰ W.-C. Yang,⁴⁵ T. Yasuda,⁵⁰ Y. A. Yatsunenko,³⁷ Z. Ye,⁵⁰ H. Yin,⁷ K. Yip,⁷³ H. D. Yoo,⁷⁷
 S. W. Youn,⁵⁰ J. Yu,⁷⁸ C. Zeitnitz,²⁷ S. Zelitch,⁸¹ T. Zhao,⁸² B. Zhou,⁶⁴ J. Zhu,⁷² M. Zielinski,⁷¹ D. Ziemska,⁵⁴
 L. Zivkovic,⁷⁰ V. Zutshi,⁵² and E. G. Zverev³⁹

(The DØ Collaboration)

¹Universidad de Buenos Aires, Buenos Aires, Argentina

²LAFEX, Centro Brasileiro de Pesquisas Físicas, Rio de Janeiro, Brazil

³Universidade do Estado do Rio de Janeiro, Rio de Janeiro, Brazil

⁴Universidade Federal do ABC, Santo André, Brazil

⁵Instituto de Física Teórica, Universidade Estadual Paulista, São Paulo, Brazil

⁶University of Alberta, Edmonton, Alberta, Canada;

Simon Fraser University, Burnaby, British Columbia, Canada;

York University, Toronto, Ontario, Canada

and McGill University, Montreal, Quebec, Canada

⁷University of Science and Technology of China, Hefei, People's Republic of China

⁸Universidad de los Andes, Bogotá, Colombia

⁹Center for Particle Physics, Charles University, Faculty of Mathematics and Physics, Prague, Czech Republic

¹⁰Czech Technical University in Prague, Prague, Czech Republic

¹¹Center for Particle Physics, Institute of Physics, Academy of Sciences of the Czech Republic, Prague, Czech Republic

¹²Universidad San Francisco de Quito, Quito, Ecuador

¹³LPC, Université Blaise Pascal, CNRS/IN2P3, Clermont, France

¹⁴LPSC, Université Joseph Fourier Grenoble 1, CNRS/IN2P3, Institut National Polytechnique de Grenoble, Grenoble, France

¹⁵CPPM, Aix-Marseille Université, CNRS/IN2P3, Marseille, France

¹⁶LAL, Université Paris-Sud, IN2P3/CNRS, Orsay, France

¹⁷LPNHE, IN2P3/CNRS, Universités Paris VI and VII, Paris, France

¹⁸CEA, Irfu, SPP, Saclay, France

¹⁹IPHC, Université de Strasbourg, CNRS/IN2P3, Strasbourg, France

²⁰IPNL, Université Lyon 1, CNRS/IN2P3, Villeurbanne, France and Université de Lyon, Lyon, France

²¹III. Physikalisches Institut A, RWTH Aachen University, Aachen, Germany

²²Physikalisches Institut, Universität Bonn, Bonn, Germany

²³Physikalisches Institut, Universität Freiburg, Freiburg, Germany

²⁴II. Physikalisches Institut, Georg-August-Universität Göttingen, Göttingen, Germany

²⁵Institut für Physik, Universität Mainz, Mainz, Germany

²⁶Ludwig-Maximilians-Universität München, München, Germany

²⁷Fachbereich Physik, University of Wuppertal, Wuppertal, Germany

²⁸Panjab University, Chandigarh, India

²⁹Delhi University, Delhi, India

³⁰Tata Institute of Fundamental Research, Mumbai, India

³¹University College Dublin, Dublin, Ireland

³²Korea Detector Laboratory, Korea University, Seoul, Korea

³³SungKyunKwan University, Suwon, Korea

³⁴CINVESTAV, Mexico City, Mexico

³⁵FOM-Institute NIKHEF and University of Amsterdam/NIKHEF, Amsterdam, The Netherlands

³⁶Radboud University Nijmegen/NIKHEF, Nijmegen, The Netherlands

³⁷Joint Institute for Nuclear Research, Dubna, Russia

³⁸Institute for Theoretical and Experimental Physics, Moscow, Russia

³⁹Moscow State University, Moscow, Russia

- ⁴⁰Institute for High Energy Physics, Protvino, Russia
⁴¹Petersburg Nuclear Physics Institute, St. Petersburg, Russia
⁴²Stockholm University, Stockholm, Sweden, and Uppsala University, Uppsala, Sweden
⁴³Lancaster University, Lancaster, United Kingdom
⁴⁴Imperial College London, London SW7 2AZ, United Kingdom
⁴⁵The University of Manchester, Manchester M13 9PL, United Kingdom
⁴⁶University of Arizona, Tucson, Arizona 85721, USA
⁴⁷California State University, Fresno, California 93740, USA
⁴⁸University of California, Riverside, California 92521, USA
⁴⁹Florida State University, Tallahassee, Florida 32306, USA
⁵⁰Fermi National Accelerator Laboratory, Batavia, Illinois 60510, USA
⁵¹University of Illinois at Chicago, Chicago, Illinois 60607, USA
⁵²Northern Illinois University, DeKalb, Illinois 60115, USA
⁵³Northwestern University, Evanston, Illinois 60208, USA
⁵⁴Indiana University, Bloomington, Indiana 47405, USA
⁵⁵University of Notre Dame, Notre Dame, Indiana 46556, USA
⁵⁶Purdue University Calumet, Hammond, Indiana 46323, USA
⁵⁷Iowa State University, Ames, Iowa 50011, USA
⁵⁸University of Kansas, Lawrence, Kansas 66045, USA
⁵⁹Kansas State University, Manhattan, Kansas 66506, USA
⁶⁰Louisiana Tech University, Ruston, Louisiana 71272, USA
⁶¹University of Maryland, College Park, Maryland 20742, USA
⁶²Boston University, Boston, Massachusetts 02215, USA
⁶³Northeastern University, Boston, Massachusetts 02115, USA
⁶⁴University of Michigan, Ann Arbor, Michigan 48109, USA
⁶⁵Michigan State University, East Lansing, Michigan 48824, USA
⁶⁶University of Mississippi, University, Mississippi 38677, USA
⁶⁷University of Nebraska, Lincoln, Nebraska 68588, USA
⁶⁸Princeton University, Princeton, New Jersey 08544, USA
⁶⁹State University of New York, Buffalo, New York 14260, USA
⁷⁰Columbia University, New York, New York 10027, USA
⁷¹University of Rochester, Rochester, New York 14627, USA
⁷²State University of New York, Stony Brook, New York 11794, USA
⁷³Brookhaven National Laboratory, Upton, New York 11973, USA
⁷⁴Langston University, Langston, Oklahoma 73050, USA
⁷⁵University of Oklahoma, Norman, Oklahoma 73019, USA
⁷⁶Oklahoma State University, Stillwater, Oklahoma 74078, USA
⁷⁷Brown University, Providence, Rhode Island 02912, USA
⁷⁸University of Texas, Arlington, Texas 76019, USA
⁷⁹Southern Methodist University, Dallas, Texas 75275, USA
⁸⁰Rice University, Houston, Texas 77005, USA
⁸¹University of Virginia, Charlottesville, Virginia 22901, USA
⁸²University of Washington, Seattle, Washington 98195, USA

(Received 4 December 2009; published 14 April 2010)

We report results from a search for production of a neutral Higgs boson in association with a b quark. We search for Higgs decays to τ pairs with one τ subsequently decaying to a muon and the other to hadrons. The data correspond to 2.7 fb^{-1} of $p\bar{p}$ collisions recorded by the D0 detector at $\sqrt{s} = 1.96 \text{ TeV}$. The data are found to be consistent with background predictions. The result allows us to exclude a significant region of parameter space of the minimal supersymmetric model.

DOI: 10.1103/PhysRevLett.104.151801

PACS numbers: 14.80.Da, 12.60.Fr, 12.60.Jv, 13.85.Rm

The current model of physics at high energies, the standard model (SM), has withstood increasingly precise experimental tests, although the Higgs boson needed to mediate the breaking of electroweak symmetry [1] has not been found. Despite the success of the SM, it has several shortcomings. Theories invoking a new fermion-boson symmetry, called supersymmetry [2] (SUSY), provide an

attractive means to address the hierarchy problem, nonunification of couplings at high energy, and offer a dark matter candidate. In addition to new SUSY-specific partners to SM particles, these theories have an extended Higgs sector. In the minimal supersymmetric standard model (MSSM), there are two Higgs doublet fields which result in five physical Higgs bosons: two neutral scalars (h, H), a

neutral pseudoscalar (A), and two charged Higgs bosons (H^\pm). The mass spectrum of the Higgs bosons is determined at tree level by two parameters, typically chosen to be $\tan\beta$, the ratio of the vacuum expectation values of up-type and down-type scalar fields and M_A , the mass of the physical pseudoscalar. Higher order corrections to the masses and couplings are dominated by the Higgsino mass parameter μ and the mixing of scalar top quarks.

In this Letter, we present a search for neutral Higgs bosons (collectively denoted ϕ) produced in association with a b quark. The specific Higgs boson decay mode used in this search is $\phi \rightarrow \tau\tau$ with one of the τ leptons subsequently decaying via $\tau \rightarrow \mu\nu_\tau\nu_\mu$ (denoted τ_μ) and the second via $\tau \rightarrow$ hadrons + ν_τ (denoted τ_h). In the MSSM, the A coupling to down-type fermions is enhanced by a factor $\propto \tan\beta$, and thus the Higgs production cross section is enhanced by a factor $\propto \tan^2\beta$ relative to the SM, giving potentially detectable rates at the Tevatron. Two of the three neutral Higgs bosons have nearly degenerate masses over much of the parameter space, effectively giving another factor of 2 in production rate. A previous search in this final state was carried out by the D0 experiment [3]. Searches in the complementary channels $\phi Z/\phi\phi \rightarrow b\bar{b}\tau\tau$, $\tau\tau b\bar{b}$ [4], $\phi \rightarrow \tau\tau$ [5,6], and $\phi b \rightarrow bbb$ [7,8] have also been carried out by the LEP, D0, and CDF experiments. By searching in complementary channels, we reduce overall sensitivity to the particular details of the model. The $b\tau\tau$ final state is less sensitive to SUSY radiative corrections than the $b\bar{b}b$ final state, and has greater sensitivity at low Higgs boson mass than the $\phi \rightarrow \tau\tau$ channel, as the b jet in the final state reduces the $Z \rightarrow \tau\tau$ background. Furthermore, an additional complementary channel will contribute to an even stronger exclusion when combining different searches. The result presented in this Letter uses an integrated luminosity of 2.7 fb^{-1} which is 8 times that used for the previous result in this channel. Because of analysis improvements, the gain in sensitivity compared to the prior result is greater than expected from the increased integrated luminosity only. We also extend the Higgs boson mass search range relative to the previous result in this channel.

The D0 detector [9] is a general purpose detector located at Fermilab's Tevatron $p\bar{p}$ collider. The Tevatron operates at a center of mass energy of 1.96 TeV . This analysis relies on all aspects of the detector: tracking, calorimetry, muon detection, the ability to identify detached vertices, and the luminosity measurement.

This search requires reconstruction of muons, hadronic τ decays, jets (arising from b quarks), and neutrinos. Muons are identified using track segments in the muon system and are required to have a track reconstructed in the inner tracking system which is close to the muon-system track segment in η and φ . Here, η is the pseudorapidity, and φ is the azimuthal angle in the plane perpendicular to the beam. Jets are reconstructed from calorimeter informa-

tion using the D0 Run II cone algorithm [10] with a radius of $R = 0.5$ in (y, φ) space, where $R = \sqrt{(\Delta y)^2 + (\Delta\varphi)^2}$ and y is the rapidity. Jets are additionally identified as being consistent with decay of a b -flavored hadron (b tagged) if the tracks aligned with the calorimeter jet have high impact parameter or form a vertex separated from the primary interaction point in the plane transverse to the beam as determined by a neural network (NN_b) algorithm [11]. Hadronic τ decays are identified [12] as clusters of energy in the calorimeter reconstructed [10] using a cone algorithm of radius $R = 0.3$ which have associated tracks. The τ candidates are then categorized as being one of three types which correspond roughly to one-prong τ decay with no π^0 's (called Type 1), one-prong decay with π^0 's (Type 2) and multiprong decay (Type 3). A final identification requirement is based on the output value of a neural network (NN_τ) designed to separate τ leptons from jets. The missing transverse energy \cancel{E}_T is used to infer the presence of neutrinos. The \cancel{E}_T is the negative of the vector sum of the transverse energy of calorimeter cells satisfying $|\eta| < 3.2$. We correct the \cancel{E}_T for the energy scales of reconstructed final state objects, including muons.

Signal acceptance and efficiency are modeled using simulated SM ϕb events generated with the PYTHIA event generator [13] requiring the b quark to satisfy $p_T > 15 \text{ GeV}/c$ and $|\eta| < 5.0$ and using the CTEQ6L1 [14] parton distribution functions (PDF). The TAUOLA [15] program is used to model τ decay, and EVTGEN [16] is used to decay b hadrons. The dependence of the Higgs boson decay width on $\tan\beta$ is included by reweighting PYTHIA samples, and the kinematic properties are reweighted to the prediction of the next-to-leading order (NLO) program MCFM [17]. The generator outputs are passed through a detailed detector simulation based on GEANT [18]. Each GEANT event is combined with collider data events recorded during a random beam crossing to model the effects of detector noise, pileup, and additional $p\bar{p}$ interactions. The combined output is then passed to the D0 event reconstruction program. Simulated signal samples are generated for different Higgs masses ranging from 90 to $320 \text{ GeV}/c^2$.

Backgrounds to this search are dominated by $Z +$ jets, $t\bar{t}$, and multijet (MJ) production. In the MJ background, the apparent leptons primarily come from semileptonic b hadron decays, not τ decays. Additional backgrounds include $W +$ jets events, SM diboson production, and single top quark production. Except for the MJ contribution, all background yields are estimated using simulated events, with the same processing chain used for signal events. The $Z +$ jets, $W +$ jets, and $t\bar{t}$ samples are generated using ALPGEN [19] with PYTHIA used for fragmentation. The diboson samples are generated using PYTHIA. For simulated samples in which there is only one lepton arising from the decay of a W boson or from $t\bar{t} \rightarrow \ell +$ jets, the second lepton is either a jet misidentified as a τ or a

muon + jet system from heavy flavor decay in which the muon is misidentified as being isolated from other activity.

Corrections accounting for differences between data and the simulation are applied to the simulated events. The corrections are derived from control data samples and applied to object identification efficiencies, trigger efficiencies, primary $p\bar{p}$ interaction position (primary vertex), and the transverse momentum spectrum of Z bosons. After applying all corrections, the yields for signal and each background are calculated as the product of the acceptance times efficiency determined from simulation, luminosity, and predicted cross sections.

The initial analysis step is a selection of events recorded by at least one trigger from a set of single muon triggers for data taken before the summer of 2006. For data taken after summer 2006, we require at least one trigger from a set of single muon triggers and muon plus hadronic τ triggers. The average trigger efficiency for signal events is approximately 65% for both data epochs.

After making the trigger requirements, a background-dominated pretag sample is selected by requiring a reconstructed primary vertex for the event with at least three tracks, exactly one reconstructed hadronic τ , exactly one isolated muon, and at least one jet. This analysis requires the τ candidates to satisfy $E_T^\tau > 10 \text{ GeV}$, $p_T^\tau > 7(5) \text{ GeV}/c$, and $NN_\tau > 0.9$ for Type 1(2) tau leptons, $E_T^\tau > 15 \text{ GeV}$, $p_T^\tau > 10 \text{ GeV}/c$, and $NN_\tau > 0.95$ for Type 3 tau leptons. Here, E_T^τ is the transverse energy of the τ measured in the calorimeter, p_T^τ is the transverse momentum sum of the associated track(s). These NN_τ requirements have an efficiency of $\approx 65\%$ in signal events and a misclassification probability of $\approx 1\%$ in multijet events. The muon must satisfy $p_T^\mu > 12 \text{ GeV}/c$ and $|\eta| < 2.0$. It is also required to be isolated from activity in the tracker and calorimeter [20]. Selected jets have $E_T > 15 \text{ GeV}$, $|\eta| < 2.5$. The τ , the muon, and jets must all be consistent with arising from the same primary vertex and be separated from each other by $\Delta R > 0.5$. In addition, the muon and τ are required to have opposite charge, and the (μ, \not{E}_T) mass variable $M \equiv \sqrt{2\not{E}_T E_\mu^2 / p_T^\mu \{1 - \cos[\Delta\varphi(\mu, \not{E}_T)]\}}$ must satisfy $M < 80$, < 80 , $< 60 \text{ GeV}/c^2$ for events with τ 's of Type 1, 2, and 3, respectively. Here, E_μ is the energy of the muon, and $\Delta\varphi$ is the opening angle between the \not{E}_T and muon in the plane transverse to the beam direction.

A more restrictive b -tag subsample with improved signal to background ratio is defined by demanding that at least one jet in each event is consistent with b -quark production [11]. The b -jet identification efficiency in signal events is about 35%, and the probability to misidentify a light jet as a b jet is 0.5%. Approximately 94% of the b -tag sample has at least one true heavy flavor jet.

All backgrounds except MJ are derived from simulated events as described earlier. The MJ background is derived from control data samples. A parent MJ-enriched control

sample is created by requiring a muon, τ , and jet as above, but with the muon isolation requirement removed and with a lower quality ($0.3 \leq NN_\tau \leq 0.9$) τ selected. This is then used to create a b -tag subsample which requires at least one of the jets to be identified as a b jet with the same b -jet selection as earlier. The residual contributions from SM backgrounds are subtracted from the MJ control samples using simulated events.

To determine the MJ contribution in the pretag analysis sample, a data sample is used that has the same selection as the pretag analysis sample except that the muon and τ charges have the same sign. This same-sign (SS) sample is dominated by MJ events. After making a subtraction of other SM background processes which contribute to this sample, the number of MJ events in the opposite-sign (OS) signal region is computed by multiplying the SS sample by the OS:SS ratio, 1.05 ± 0.02 , determined in a control sample selected by requiring a nonisolated muon.

For the b -tag analysis sample, statistical limitations require a different approach for the MJ background evaluation than for the pretag sample. For the b -tag sample, two methods are used. For the first method, the per jet probability P_{tag} that a jet in the SS MJ control subsample would be identified as a b jet is determined as a function of jet p_T . We apply P_{tag} to the jets in the SS pretag sample to determine the yield in the b -tag sample. For the second method, the MJ background is determined by multiplying the b -tag MJ control sample yield by two factors: (1) the probability that the nonisolated muon would be identified as isolated, and (2) the ratio of events with a τ candidate passing the NN_τ requirements to events with τ candidates having $0.3 \leq NN_\tau < 0.9$ as determined in a separate control sample. The final MJ contribution in the b -tag analysis sample is determined using the MJ shape from the first method with the normalization equal to the average of the two methods. We include the normalization difference between the two methods in the systematic uncertainty on the MJ contribution.

TABLE I. Predicted background yield, observed data yield, and predicted signal yield and their statistical uncertainties at three stages of the analysis. The signal yields are based on the sum of all neutral Higgs bosons assuming $\tan\beta = 40$ and $M_A = 120 \text{ GeV}/c^2$ for the m_h^{\max} and $\mu = -200 \text{ GeV}/c^2$ scenario. The total background uncertainty at the Final analysis stage including systematic uncertainties is 8.4 events.

	Pretag	b tagged	Final
$t\bar{t}$	66.0 ± 1.3	39.6 ± 0.8	20.3 ± 0.6
Multijet	549 ± 26	38.5 ± 2.3	28.1 ± 1.9
$Z(\rightarrow \tau\tau) + \text{jets}$	1241 ± 8	18.8 ± 0.3	16.3 ± 0.3
Other Bkg	267 ± 6	5.1 ± 0.1	4.1 ± 0.1
Total Bkg	2123 ± 28	102 ± 2.4	68.7 ± 2.0
Data	2077	112	79
Signal	26.5 ± 0.3	8.8 ± 0.1	8.4 ± 0.1

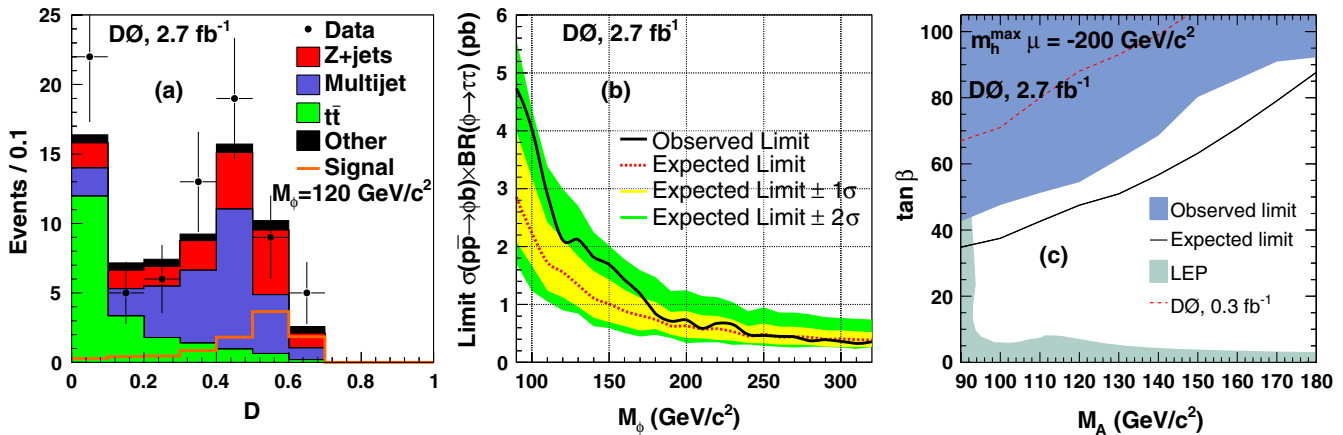


FIG. 1 (color online). (a) The distribution of the final discriminant variable, $D = \text{NN}_{\text{top}} \times \text{LL}_{\text{MJ}}$. The figure includes all τ types. (b) The cross-section limit as a function of Higgs boson mass. (c) The region in the $\tan \beta$ versus M_A plane excluded by this analysis, LEP neutral MSSM Higgs searches, and the previous D0 result in this channel.

The signal to background ratio is further improved using multivariate techniques. Two separate methods are used, one to address the $t\bar{t}$ background and one to reduce the MJ background. For the $t\bar{t}$ background, a neural network (NN_{top}) is constructed using $H_T \equiv \sum_{\text{jets}} E_T$, $E_{\text{tot}} \equiv \sum_{\text{jets}} E + E_\tau + E_\mu$, the number of jets and $\Delta\varphi(\mu, \tau)$ as inputs. For the MJ background, a simple joint likelihood discriminant (LL_{MJ}) is constructed using p_T^μ , p_T^τ , $\Delta R(\mu, \tau)$, $M_{\mu\tau}$, and $M_{\mu\tau\nu}$. Here, $M_{\mu\tau}$ denotes the invariant mass of the muon and tau, and $M_{\mu\tau\nu}$ is the invariant mass computed from the muon, τ , and \cancel{E}_T momentum vectors. The final analysis sample is defined by selecting rectangular regions in the NN_{top} versus LL_{MJ} plane. The regions have been identified for each τ type and each Higgs boson mass point separately by optimizing the search sensitivity using simulated events. The signal to background ratio improves by up to a factor of 2 when applying these requirements.

Table I shows the predicted background and observed data yields in the analysis samples. The selection efficiency for signal events varies between 5% and 10% depending on M_ϕ .

Systematic uncertainties arise from a variety of sources. Most are evaluated using comparisons between data control samples and predictions from simulation. The uncertainties are divided into two categories: (1) those which affect only normalization, and (2) those which also affect the shape of distributions. The sources in the first category include the luminosity (6.1%), muon identification efficiency (4.5%), τ_h identification (5%, 4%, 8%), τ_h energy calibration (3%), the $t\bar{t}$ and single top cross sections (11% and 12%), diboson cross sections (6%), $Z + (u, d, s, c)$ rate (+2%, -5%), and the $W + b$ and $Z + b$ cross sections (30%); those in the second include jet energy calibration (2%-4%), b -tagging (3%-5%), trigger (3%-5%), and MJ background (33%, 12%, 11%). For sources with three

values, the values correspond to τ Types 1, 2, and 3, respectively.

After making the final selection, the discriminant D is formed from the product of the NN_{top} and LL_{MJ} variables, $D = \text{LL}_{\text{MJ}} \times \text{NN}_{\text{top}}$. The resulting distributions for the predicted background, signal, and data are shown in Fig. 1(a). This distribution is used as input to a significance calculation using a modified frequentist approach with a Poisson log-likelihood ratio test statistic [21]. In the absence of a significant signal, we set 95% confidence level limits on the presence of neutral Higgs bosons in our data sample. The cross-section limits are shown in Fig. 1(b) as a function of Higgs boson mass. We translate them into the $\tan \beta$ versus M_A plane in several MSSM benchmark scenarios [22–24], including the $m_h^{\max}, \mu = -200 \text{ GeV}/c^2$ scenario shown in Fig. 1(c). Results for other scenarios are in [25]. The signal cross sections and branching fractions are computed using FEYNHIGGS [26]. Instabilities in the theoretical calculation for $\tan \beta > 100$ limit the usable mass range in the translation into the $(\tan \beta, M_A)$ plane.

In summary, this Letter reports a search for production of Higgs bosons in association with a b quark using 8 times more data than previous results for this channel. The data are consistent with predictions from known physics sources and limits are set on the neutral Higgs boson associated production cross section. These cross-section limits, a factor of 3 improvement over previous results, are also translated into limits in the SUSY parameter space.

We thank the staffs at Fermilab and collaborating institutions, and acknowledge support from the DOE and NSF (USA); CEA and CNRS/IN2P3 (France); FASI, Rosatom and RFBR (Russia); CNPq, FAPERJ, FAPESP and FUNDUNESP (Brazil); DAE and DST (India); Colciencias (Colombia); CONACyT (Mexico); KRF and KOSEF (Korea); CONICET and UBACyT (Argentina); FOM (The Netherlands); STFC and the Royal Society

(United Kingdom); MSMT and GACR (Czech Republic); CRC Program, CFI, NSERC and WestGrid Project (Canada); BMBF and DFG (Germany); SFI (Ireland); The Swedish Research Council (Sweden); and CAS and CNSF (China).

^{*}Visitor from Augustana College, Sioux Falls, SD, USA.

[†]Visitor from Rutgers University, Piscataway, NJ, USA.

[‡]Visitor from The University of Liverpool, Liverpool, UK.

[§]Visitor from SLAC, Menlo Park, CA, USA.

^{||}Visitor from Centro de Investigacion en Computacion - IPN, Mexico City, Mexico.

[¶]Visitor from ECFM, Universidad Autonoma de Sinaloa, Culiacán, Mexico.

^{**}Visitor from Universität Bern, Bern, Switzerland.

^{††}Visitor from Universität Zürich, Zürich, Switzerland.

- [1] A. Djouadi, *Phys. Rep.* **457**, 1 (2008); A. Djouadi, *Phys. Rep.* **459**, 1 (2008); and references therein.
- [2] H. P. Nilles, *Phys. Rep.* **110**, 1 (1984); H. E. Haber and G. L. Kane, *Phys. Rep.* **117**, 75 (1985).
- [3] V. M. Abazov *et al.* (D0 Collaboration), *Phys. Rev. Lett.* **102**, 051804 (2009).
- [4] The LEP Working Group for Higgs Boson Searches, ALEPH Collaboration, DELPHI Collaboration, L3 Collaboration, and OPAL Collaboration, *Eur. Phys. J. C* **47**, 547 (2006).
- [5] V. M. Abazov *et al.* (D0 Collaboration), *Phys. Rev. Lett.* **101**, 071804 (2008).
- [6] A. Abulencia *et al.* (CDF Collaboration), *Phys. Rev. Lett.* **96**, 011802 (2006).
- [7] V. M. Abazov *et al.* (D0 Collaboration), *Phys. Rev. Lett.* **101**, 221802 (2008).
- [8] T. Affolder *et al.* (CDF Collaboration), *Phys. Rev. Lett.* **86**, 4472 (2001).
- [9] V. M. Abazov *et al.* (D0 Collaboration), *Nucl. Instrum. Methods Phys. Res., Sect. A* **565**, 463 (2006).
- [10] G. Blazey *et al.*, arXiv:hep-ex/0005012.
- [11] V. M. Abazov *et al.* (D0 Collaboration), arXiv:1002.4224 [Nucl. Instrum. Methods in Phys. Res. A (to be published)].
- [12] V. M. Abazov *et al.* (D0 Collaboration), *Phys. Lett. B* **670**, 292 (2009).
- [13] T. Sjöstrand *et al.*, *Comput. Phys. Commun.* **135**, 238 (2001). Version 6.409.
- [14] J. Pumplin *et al.*, *J. High Energy Phys.* 07 (2002) 012; D. Stump *et al.*, *J. High Energy Phys.* 10 (2003) 046.
- [15] Z. Was, *Nucl. Phys. B, Proc. Suppl.* **98**, 96 (2001). Version 2.5.04.
- [16] D. J. Lange, *Nucl. Instrum. Methods Phys. Res., Sect. A* **462**, 152 (2001). Version 9.39.
- [17] J. Campbell and R. K. Ellis, *Phys. Rev. D* **65**, 113007 (2002). Version 5.6.
- [18] R. Brun and F. Carminati, CERN Program Library Long Writeup, Report No. W5013, 1993 (unpublished), Version 3.21.
- [19] M. L. Mangano, M. Moretti, F. Piccinini, R. Pittau, and A. Polosa, *J. High Energy Phys.* 07 (2003) 001. Version 2.11.
- [20] V. M. Abazov *et al.* (D0 Collaboration), *Phys. Rev. Lett.* **93**, 141801 (2004).
- [21] W. Fisher, FERMILAB Report No. FERMILAB-TM-2386-E, 2007.
- [22] M. Carena, S. Heinemeyer, C. E. M. Wagner, and G. Weiglein, *Eur. Phys. J. C* **45**, 797 (2006).
- [23] M. Carena, S. Heinemeyer, C. E. M. Wagner, and G. Weiglein, *Eur. Phys. J. C* **26**, 601 (2003).
- [24] S. Heinemeyer, W. Hollik, and G. Weiglein, *J. High Energy Phys.* 6 (2000) 009.
- [25] See supplementary material at <http://link.aps.org/supplemental/10.1103/PhysRevLett.104.151801> for additional tables and figures including results for other MSSM benchmark scenarios.
- [26] M. Frank, T. Hahn, S. Heinemeyer, W. Hollik, H. Rzebak, and G. Weiglein, *J. High Energy Phys.* 02 (2007) 47. Version 2.6.5; G. Degrassi, S. Heinemeyer, W. Hollik, P. Slavich, and G. Weiglein, *Eur. Phys. J. C* **28**, 133 (2003); S. Heinemeyer, W. Hollik, and G. Weiglein, *Eur. Phys. J. C* **9**, 343 (1999); S. Heinemeyer, W. Hollik, and G. Weiglein, *Comput. Phys. Commun.* **124**, 76 (2000).